Science Advances
AAAS

advances.sciencemag.org/cgi/content/full/6/33/eabb4922/DC1

Supplementary Materials for

Decades-old model of slow adaptation in sensory hair cells is not supported in mammals

Giusy A. Caprara, Andrew A. Mecca, Anthony W. Peng*

*Corresponding author. Email: anthony.peng@cuanschutz.edu

Published 14 August 2020, *Sci. Adv.* **6**, eabb4922 (2020)
DOI: 10.1126/sciadv.abb4922

This PDF file includes:

Figs. S1 to S6

Supplemental Figures

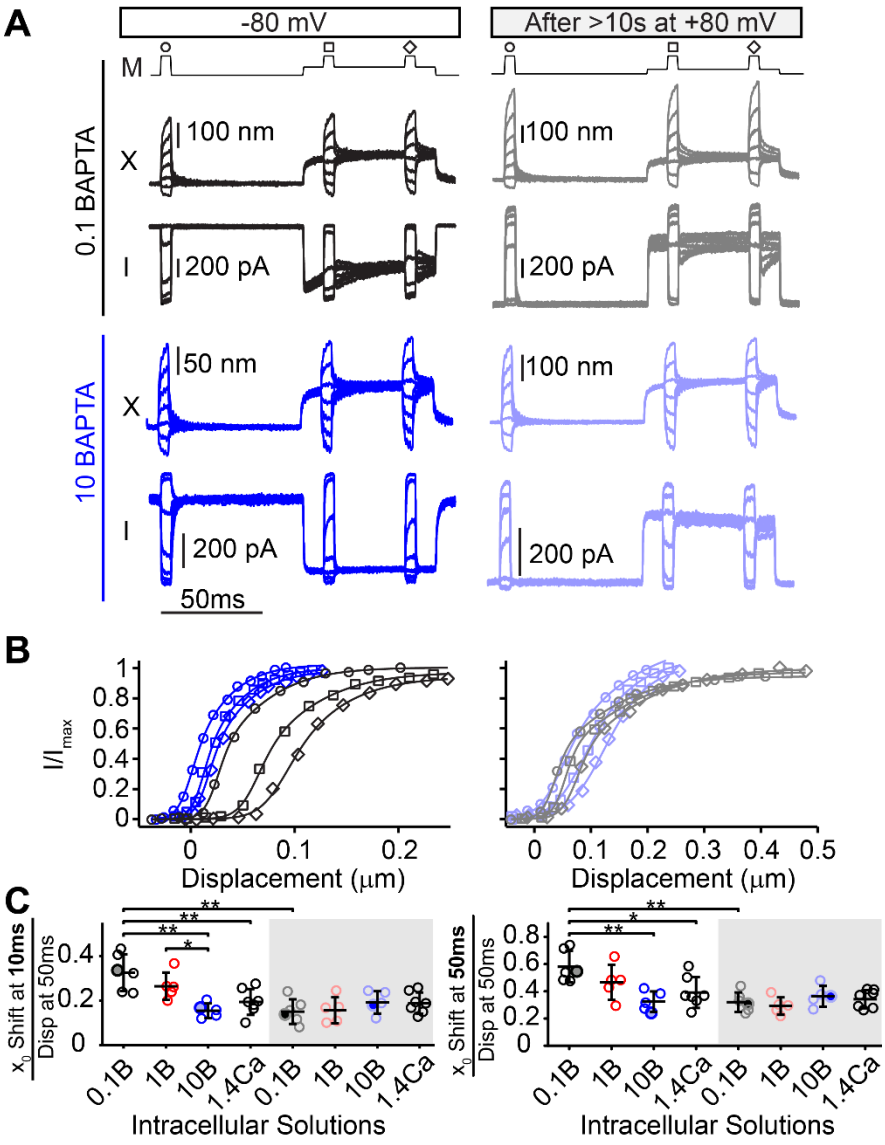

Figure S1. Intracellular Ca^{2+} buffering modulates the activation curve shift in a multi-pulse experiment. **A**, family of bundle displacements (X) and currents (I) recorded at negative (-80 mV, darker traces) and positive (+80 mV, lighter traces) potentials with two different intracellular BAPTA concentrations: 0.1 mM (black), and 10 mM (blue). M shows the timing of the fluid-jet stimulus waveform with symbols used in B where the activation curves are measured. **B**, family of activation curves generated from the cells shown in A. Adaptation manifests as a right shift of the second (at 10 ms, squares) and third activation (at 50 ms, diamonds) curves with respect to the first (circles). **C**, summary plots of the X_0 shift at 10 ms (left plot) and at 50 ms (right plot) with different intracellular solutions at negative and positive (gray shading) potentials. All data are normalized to the measured bundle displacement just before the test pulse at 50 ms. The cells shown in A are marked with filled circles. Black bars represent mean ± SD. Paired Student's t-tests were performed for the data in each internal solution between -80 and +80 holding potentials. Unpaired, unequal variance Student's t-tests were used to compare amongst all intracellular solutions at -80 and separately at +80. * $p \leq 0.05$. ** $p \leq 0.01$. Number of cells (animals): 0.1 BAPTA - 6 (6), 1 BAPTA - 5 (5), 10 BAPTA - 5 (5), 1.4 Ca - 7 (7).

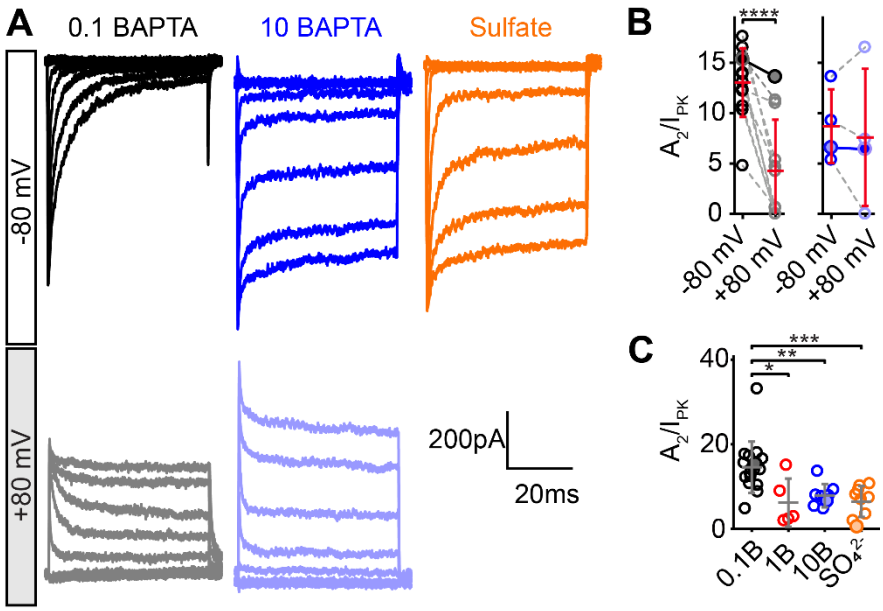

Figure S2. Slow Ca^{2+}-dependent adaptation is also visible with rigid probe stimulation. **A**, family of currents elicited from a 50 ms step-like displacement delivered with rigid probe and recorded with an intracellular concentration of 0.1 mM BAPTA (black trace), 10 mM BAPTA (blue trace), and 0.1 mM BAPTA + 60 mM Cs_2SO_4 (orange trace) at negative (darker traces) and positive (lighter traces) potentials. The current decays with two-time constants with the slower time constant representing slow adaptation. The magnitude of the slower decay decreases with higher intracellular BAPTA concentration, myosin ATPase inhibitor, or depolarization to +80 mV. **B**, summary plots of the maximum relative magnitude of slow adaptation at negative (-80 mV) and positive (+80 mV) potentials with an intracellular concentration of 0.1 mM BAPTA (left plot) and 10 mM BAPTA (right plot). Dashed lines connect data points for a given cell. Cells shown in A are marked with filled symbols. **C**, summary plot of the maximum relative magnitude of slow adaptation in cells recorded with an intracellular concentration of 0.1 mM BAPTA (0.1B, black), 1 mM BAPTA (1B, red), 10 mM BAPTA (10B, blue), and 0.1 mM BAPTA + 60 mM Cs_2SO_4 (SO_4^{2-}, orange). The differences in the slow adaptation recorded with a rigid probe stimulation are comparable with the differences of the adaptation magnitude recorded with the fluid-jet stimulation. Error bars represent mean ± SD. * $p \leq 0.05$. ** $p \leq 0.01$. *** $p \leq 0.001$. **** $p \leq 0.0001$. Number of cells (animals): for panel B, 0.1 BAPTA - 12 (9), 10 BAPTA - 4 (3); for panel C, 0.1 BAPTA - 16 (11), 1 BAPTA - 5 (5), 10 BAPTA - 8 (4), Cs_2SO_4 - 9 (9).

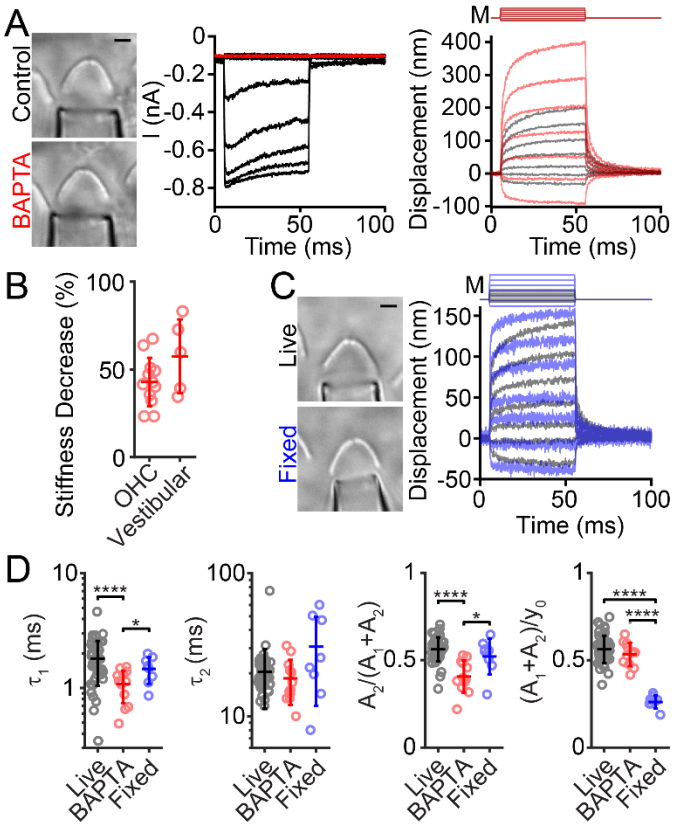

Figure S3. Ca^{2+}-chelator treatment and tissue fixation alter hair bundle creep. **A**, MET current and hair bundle motion before (black) and after treatment with 5 mM BAPTA (red) in the extracellular solution are plotted with a frame from the hair-bundle motion video on the left. M indicates the stimulus driver voltage waveform. Note that the stimulus is the same for control and after BAPTA treatment. **B**, during treatment with Ca^{2+}-chelators, the stiffness of the hair bundle decreases as seen in the displacement traces in panel A. The data show the percent decrease in stiffness for both cochlear OHCs (n=12) and vestibular hair cells (n=5) after Ca^{2+}-chelator treatment. **C**, hair bundle motion of a live cell with 1 mM BAPTA intracellular solution (gray traces) and a cell that had been fixed overnight (blue traces) are shown. Frames from the hair bundle videos are shown on the left. M indicates the stimulus driver waveforms. Note that larger fluid jet stimuli were required to elicit comparable hair-bundle displacements. **D**, double exponential fit parameters describing the hair bundle creep in OHCs are summarized. $(A_1+A_2)/y_0$ describes the relative magnitude of hair bundle creep, showing that there was less creep with fixed tissue. $A_2/(A_1+A_2)$ describes the percentage of the slower creep time constant, showing that there was a smaller contribution of the slow time constants after BAPTA treatment. Two-tailed, unpaired, unequal variance t-test was used for these data. n=22, 12, 8, for Live, BAPTA, and Fixed, respectively. Summary data for OHCs combined experiments that used BAPTA and EDTA since they yielded similar results. Scale bars = 2 µm. * $p \leq 0.05$. **** $p \leq 0.0001$

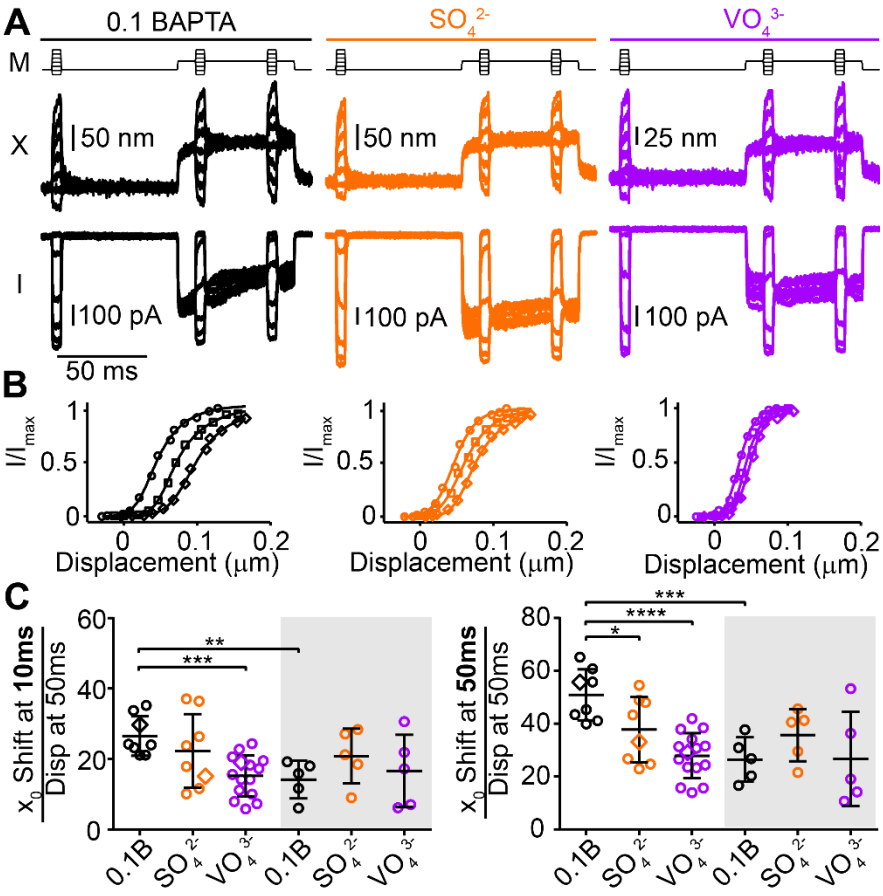

Figure S4. Inhibition of ATPases decreases activation curve shifts in a multi-pulse stimulation protocol. **A**, family of bundle displacements (X) and currents (I) recorded with 0.1 mM BAPTA intracellular concentration (black, orange and purple traces) with 60 mM cesium sulfate (Cs_2SO_4, myosin blocker - orange traces) or 4 mM sodium orthovanadate (Na_3VO_4, myosin and PMCAs blocker - purple traces) in the intracellular solution. M shows the fluid-jet stimulus waveform. **B**, family of activation curves generated from the cells shown in A. The resting activation curve (circles) is shown with activation curves after 10 ms (squares) and 50 ms (diamonds) of a sustained stimulus. The amount of shift decreases when ATPase activity is inhibited with SO_4^{2-} or VO_4^{3-}. **C**, summary plots of the X_0 shift at 10 ms (left plot) and at 50 ms (right plot) at negative and positive (gray shading) potentials. All data are normalized to the displacement at 50 ms. Cells shown in A are marked. Black error bars represent mean ± SD. * $p \leq 0.05$. ** $p \leq 0.01$. *** $p \leq 0.001$. **** $p \leq 0.0001$. Number of cells (animals): 0.1BAPTA - 8 (6), SO_4^{2-} - 8 (6), VO_4^{3-} - 15 (14).

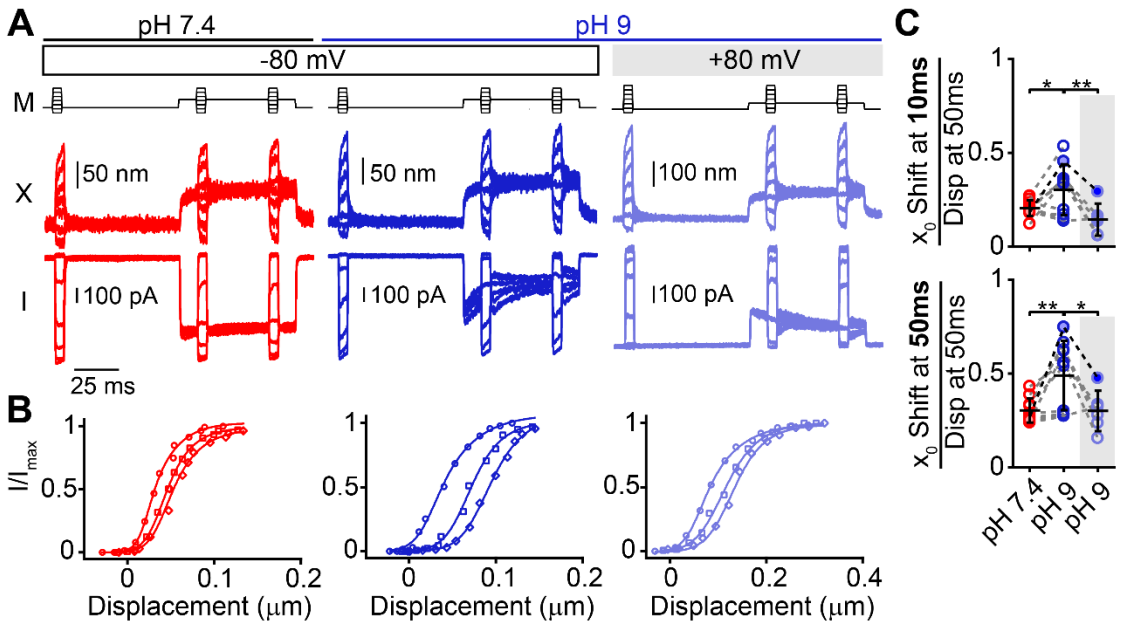

Figure S5. Inhibition of PMCA pumps increases activation curve shifts in a multi-pulse stimulation protocol. **A**, family of bundle displacements (X) and currents (I) recorded from the same cell in normal extracellular solution (pH 7.4, red traces) and after 10 minutes of PMCA inhibition (pH 9, blue traces) at negative (-80 mV) and positive (+80 mV) (lighter blue traces) potentials. M shows the fluid-jet stimulus waveform. **B**, family of activation curves generated from the cells shown in A. Adaptation manifests as a right shift of the second (at 10 ms, squares) and third activation (at 50 ms, diamonds) curves with respect to the first (circles). **C**, summary plots of the X_0 shift at 10 ms (top plot) and at 50 ms (bottom plot) before (pH 7.4, red) and after 10 minutes of PMCA inhibition (pH 9, blue) at negative and positive (gray shading) potentials. All data are normalized to the displacement at 50 ms. Cells shown in A are marked. Dashed lines connect data points for a given cell, and black error bars represent mean ± SD. * $p \leq 0.05$. ** $p \leq 0.01$. Number of cells (animals): pH 7.4 - 10 (10), pH 9 - 10 (10), +80 pH9 - 6 (6).

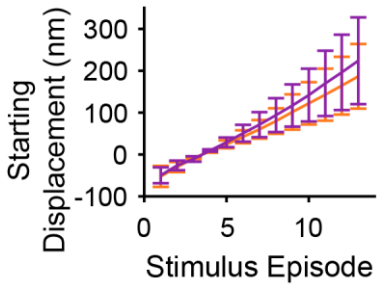

Figure S6 Cells with VO_4^{3-} appear less stiff than cells with SO_4^{2-}. Starting displacements from cells recording using 1 mM BAPTA in the intracellular solution with VO_4^{3-} (n=14, purple) and SO_4^{2-} (n=10, orange). The displacement immediately following the plateau of the force stimulus (frames 61-63) were averaged together to get the starting displacement for each stimulus episode. All cells for each condition were averaged together with the mean and standard deviation plotted. Two-way ANOVA analysis indicates that these two conditions are different (p = 0.0003).